Journal of Geodynamics 86 (2015) 1–9

Contents lists available at ScienceDirect

Journal of Geodynamics

journal homepage: http://www.elsevier.com/locate/jog

Technical note

The influence of viscosity structure in the lithosphere on predictions from models of glacial isostatic adjustment

Joseph Kuchar[a,*], Glenn A. Milne[b]

[a] Department of Physics, University of Ottawa, Ottawa, Ontario, Canada K1N 6N5
[b] Department of Earth Sciences, University of Ottawa, Ontario, Canada K1N 6N5

ARTICLE INFO

Article history:
Received 21 July 2014
Received in revised form
22 December 2014
Accepted 7 January 2015
Available online 3 February 2015

Keywords:
Glacial isostatic adjustment
Lithosphere structure
Rheology

ABSTRACT

The thickness of the lithosphere inferred in most glacial isostatic adjustment (GIA) modelling studies tends to be significantly thinner than when found through seismic or thermal modelling studies. In those GIA studies, the lithosphere tends to be modelled as a plate of uniform and very high viscosity. We develop and test Earth models that include depth-dependent viscosity in the lithosphere to consider the implications for inferring lithospheric thickness from observed relative sea-level (RSL) changes. We find that when comparing predictions of RSL between the traditional plate lithosphere models and those with viscous structure, the latter produce RSL predictions that most closely resemble those from traditional models that are 10 s of km thinner. The greatest sensitivity to this change in the Earth model is most evident in regions loaded by relatively small ice sheets such as the British Isles. We also find that the effective elastic thickness of the lithosphere models with viscous structure is time-dependent, with thinning by tens of kilometres over a timescale of ∼10 kyr.

1. Introduction

The lithosphere's response to stresses associated with various processes on a range of time scales helps shape the form of the Earth around us. The rheological structure of the lithosphere is not well determined in many regions but is essential to understand dynamical processes such as seismic and post-seismic deformation, flexure and isostatic adjustment due to surface loads (such as ice sheets and volcanos), sedimentary basin formation, and inter and intra plate deformation (e.g., Watts et al., 2013; Turcotte and Schubert, 2002). The particular property of the lithosphere that we are concerned with in this study is its thickness.

The thickness of the lithosphere has been estimated through a number of methods, including inversions of gravity and seismic observations (Audet and Mareschal, 2004) and through thermal (Tesauro et al., 2009) and geodynamic modelling – which includes glacial isostatic adjustment (GIA) modelling (Lambeck et al., 1998). The values obtained through these different methods vary widely for a given region as the thicknesses inferred relate to different properties. For example, a recent study inferred lithospheric thicknesses in Europe through seismic constraints on mantle temperatures (Tesauro et al., 2009) and by choosing the 1200 °C isotherm as defining the lithosphere-asthenosphere boundary. In the British Isles region, their inferred depth to this isotherm ranged from less than 100 km off the northwest coast of Scotland to almost 200 km in the North Sea, with an average value around 150 km. In contrast, GIA studies have inferred lithosphere thickness values of 60–90 km (Lambeck et al., 1996; Peltier et al., 2002; Bradley et al., 2009; Kuchar et al., 2012). As another example, a thermal study of the Canadian Shield (Levy et al., 2010) used surface heat flux measurements to infer the thickness of the lithosphere, and they found it varied from 200 km to 300 km. In contrast, GIA studies of the region typically adopt Earth models with lithosphere components around 120 km thick (e.g., Davis and Mitrovica, 1996; Sella et al., 2007). Finally, the effective elastic thickness (EET) of the Canadian Shield lithosphere was estimated to be 30 km to 130 km from Bouguer gravity anomaly data (Audet and Mareschal, 2004). A more detailed summary of lithosphere definitions and thickness estimates is given by Martinec and Wolf (2005), in the context of the Fennoscandian lithosphere.

The differences noted above are a reflection of the fact that the lithosphere thicknesses inferred relate to different properties or timescales. For example, the consistently low thicknesses estimated via GIA modelling are related to how the lithosphere tends to be defined in these models, which is as a region of very high and constant viscosity (often of order 10^{30} Pa s or higher), such that the lithosphere acts essentially as an elastic layer over typical GIA timescales (1–10 kyr). In this way, the inferences made via GIA

* Corresponding author. Tel.: +1 6135525728.
E-mail address: joseph.kuchar@gmail.com (J. Kuchar).

http://dx.doi.org/10.1016/j.jog.2015.01.002
0264-3707/

studies are more compatible with the EET estimates from gravity data. We note, however, that the latter tends to result in even lower thickness estimates due to the longer timescales involved when considering this approach (and consequently more time for extensive stress relaxation through ductile failure; e.g., Ranalli, 1995).

The primary goal of this study is to consider how GIA model output is affected when the lithosphere is defined with viscous structure in order to gauge how inferences of lithospheric thickness, based on the typical elastic layer approach, might be affected. More specifically, we consider whether incorporating viscous structure in the lithosphere can result in estimates of this parameter that are more in line with those made using other methods, such as the thermal modelling approach outlined above. For convenience, we refer to the high viscosity lithospheres typical in GIA studies as "elastic lithospheres," with the understanding that they are generally not modelled as being elastic, but rather as having Maxwell rheologies with very high viscosities. In this study we let the strength profile of the lithosphere be determined by temperature and composition, as described by the Dorn equation (see next section).

Previous GIA modelling studies have included lithosphere components with more structure by investigating the influence of a low viscosity region within an otherwise high viscosity lithosphere (DiDonato et al., 2000; Kendall et al., 2003; Klemann and Wolf, 1999), which resulted in a thinning of the lithosphere's EET to approximately the thickness of the lithosphere above the low viscosity zone. This differs from our own approach, which does not limit the ductile behaviour in the lithosphere to a small zone within it. Our approach is more closely aligned with that of Klemann and Wolf (1998) who estimated continuous changes in viscosity with depth associated with temperature-activated creep processes. Some recent studies have considered sub-crustal viscosity structure in the lithosphere within the context of non-linear, power-law deformation (van der Wal et al., 2013).

Additionally, it is known that the EET of the lithosphere depends on factors like the size and age of the load inducing the deformations (Watts et al., 2013), and so by incorporating more realistic viscous structure into the lithosphere we are effectively making the strength of the lithosphere time and load-size dependent. This may be an important consideration in GIA studies, where the time scales can range from thousands to tens of thousands of years and the load size from (typically) hundreds to thousands of kilometres.

2. Methodology

2.1. GIA model

In general, a GIA model has three key components: an ice history, provided in this study by ICE5G (Peltier, 2004; version 1.2); an Earth model to calculate solid Earth deformation and perturbation to the geopotential in response to the ice-ocean loading; and a sea level model that solves the sea level equation to determine how sea level changes in response to the ice loading and Earth deformation. We discuss the Earth model component in detail below. The sea level model we apply solves the generalised sea level equation (Kendall et al., 2005; Mitrovica and Milne, 2003), and therefore includes a treatment of time varying shorelines and sea level change in regions of ablating marine based ice. The influence of GIA-induced perturbations to the Earth's rotation vector on sea level is also included (Milne and Mitrovica, 1998; Mitrovica et al., 2005).

All the Earth models in this study are spherically symmetric Maxwell bodies with an elastic and density structure given by PREM (Dziewonski and Anderson, 1981). The sub-lithosphere viscous structure is defined in two regions: the upper mantle (base of lithosphere to 660 km seismic discontinuity) and the lower mantle (660 km to the core-mantle boundary); we adopt values for these respective regions of 5×10^{20} Pa s and 10^{22} Pa s. As described above, the lithosphere is commonly defined as a shell of uniform and very high viscosity – several orders of magnitude higher than that of the upper mantle. We improve upon these simplistic lithosphere models by considering variations in lithosphere strength due to changes in composition and temperature. Specifically, we assume a quartzite composition to the Mohorovicic discontinuity ("Moho") at 24.4 km depth, and a mafic granulite composition for the mantle component, with parameters given in Tesauro et al., 2009; see Table 1. We adopt a power law flow model for the lithosphere as defined by the Dorn equation,

Table 1
Parameters adopted in defining the lithosphere viscosity profiles shown in Fig. 1.

Parameter	Upper crust	Lower crust
$\dot{\varepsilon}$ (s^{-1})	10^{-15}	10^{-15}
A_D ($Pa^{-n}\,s^{-1}$)	6.03×10^{-24}	8.83×10^{-22}
n	2.72	4.2
E_D ($J\,mol^{-1}$)	134×10^3	445×10^3

$$\dot{\varepsilon} = A_D \sigma^n e^{-E_D/RT} \tag{1}$$

where $\dot{\varepsilon}$ is the strain rate and is set to $10^{-15}\,s^{-1}$, E_D is the activation enthalpy, R is the gas constant, T is temperature, and A_D and n are experimentally determined parameters that depend on the type of rock, pressure and other environmental parameters that we will neglect in this preliminary analysis. Eq. (1) can be inverted to produce an expression for stress, σ (Table 1).

It is important to note an inconsistency in our approach: the Earth component of the GIA model we are applying assumes a Maxwell rheology, which has a linear stress–strain relationship, but we are defining the viscosity-depth structure in the lithosphere derived from a non-linear relationship (Eq. (1)). In a non-linear rheology the viscosity is stress dependent, with regions of higher stress being characterised by lower (effective) viscosities. In a Maxwell model, the viscosity values are constant and stress independent. We obtain the initial viscosity profile assuming a non-linear stress–strain relationship, but it is treated in our model linearly. We chose to follow this approach for two reasons: (1) there is growing evidence that non-linear (as opposed to linear) deformation is dominant in the lithosphere (e.g., Bürgmann and Dresen, 2008) and so application of Eq. (1), as opposed to a linear relation ($n = 1$), leads to a more accurate estimate of the viscosity structure; (2) while the application of a non-linear Earth model within our GIA model would be consistent with the application of Eq. (1), this adds a second advance compared to most previous GIA modelling studies and so interpretation of the results would be less straightforward. Our aim in this study is not to investigate the effects of non-linear versus linear rheology on postglacial rebound (e.g., Wu and Wang, 2008), rather, we adopt the Dorn equation to compute a viscosity profile for the lithosphere that should more closely resemble reality than does the traditional elastic layer model adopted in most previous GIA studies.

The lithosphere viscosity profile is modelled as two ductile zones separated by a discontinuity at the Moho. The Dorn Eq. (1) requires a temperature profile, for which we assume radiogenic heat production within the lithosphere. The analytic expression for temperature that we adopt within the lithosphere is (e.g., Turcotte and Schubert, 2002),

$$T(Z) = \frac{A_0 h^2}{K}(1 - e^{-Z/h}) + \left(T_0' - \frac{A_0 h}{K}\right) Z + T_0, \tag{2}$$

where A_0 is the radiogenic heat production rate at the surface, h is a scaling parameter set to 11 km, K is the conductivity, set to a constant 3 W/mK, T_0' is the surface temperature gradient, and T_0

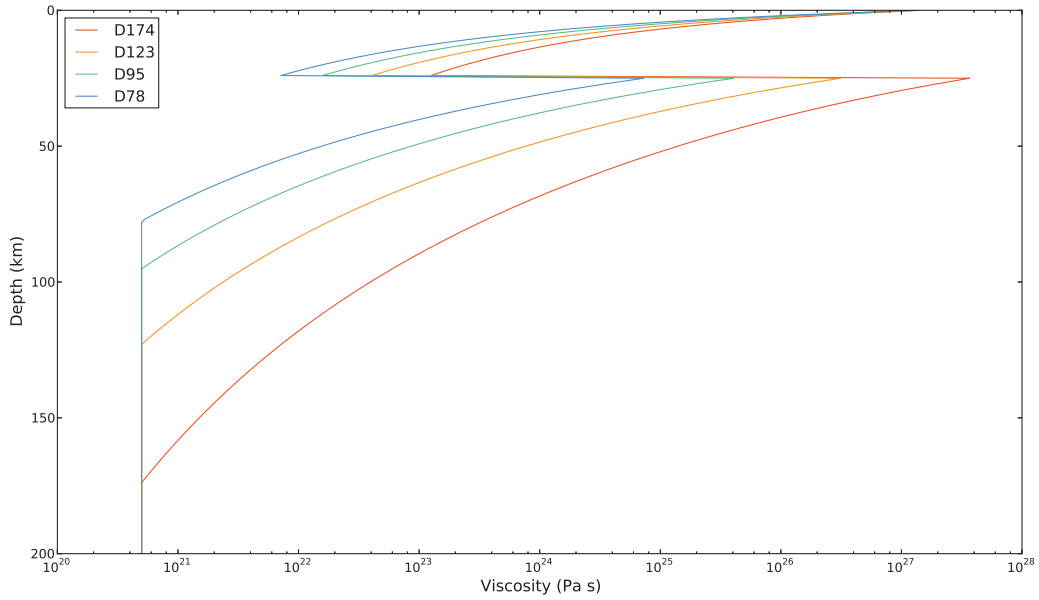

Fig. 1. Lithosphere viscosity profiles for the four Earth models described in the text. Labels in the key denote the lithospheric thickness of each model in kilometres. Note that the *x*-axis (viscosity) is plotted logarithmically.

is the temperature at the Earth's surface, assumed to be 0 °C. Our temperature profiles and thus our strength profiles are dependent on the surface temperature gradient. Note that, by applying Eq. (2), we ignore the effect of heat transfer via convection on the Earth's temperature profile. This would lead to greater temperatures and therefore lower viscosities at depth in the lithosphere. We convert our strength profiles to viscosity profiles through

$$\eta = \frac{\sigma}{2\dot{\varepsilon}} \tag{3}$$

which, when combined with Eq. (1), gives

$$\eta = \frac{1}{2}\left(\frac{\dot{\varepsilon}^{1-n}}{A_D}\right)^{1/n} \exp\left(\frac{E_D}{nRT}\right) \tag{4}$$

Eq. (4) indicates that the viscosity (for $n > 1$) will depend on stress such that regions of higher stress will exhibit lower (effective) viscosity.

We test four Earth models, with surface temperature gradients $T_0' = 14,\ 16,\ 18$, and 20 K/km, corresponding to a range of surface heat flow values of 42–60 mW/m^2. The four models are shown in Fig. 1 and their associated temperature profiles in Fig. 2. Because we assume different compositions above and below the Moho (taken to be at 24.4 km based on PREM; Dziewonski and Anderson (1981)), the calculated viscosity profile has a discontinuity at this depth.

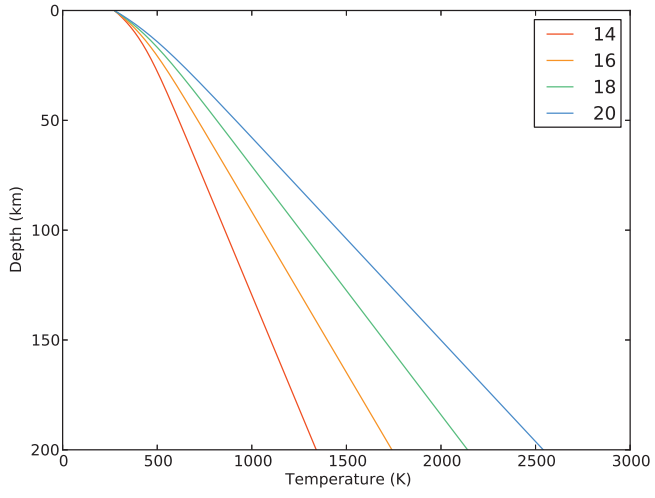

Fig. 2. Temperature profiles corresponding to the viscosity profiles shown in Fig. 1.

In traditional GIA studies, the lithosphere viscosity is much greater than that of the upper mantle and so the thickness of this region corresponds to that of an (effectively) elastic layer. Our more realistic model results in a lithosphere with a viscosity that is not, in general, many orders of magnitude greater than that of the upper mantle, and so defining an EET is less straightforward, as it will depend on the spatial and temporal scale of the loading (see Fig. 4 and related discussion). Therefore, to simplify the comparison between these two lithosphere models and more directly address the aim of this study, we chose to define a thickness of our viscosity-varying lithosphere models as the depth at which the viscosity in the component of the lithosphere between the Moho and the upper mantle drops down to the viscosity of the upper mantle (5×10^{20} Pa s). Applying this approach results in values of 174, 123, 95 and 78 km. In the following, these are referred to as D174, D123, D95 and D78 to indicate that these models can exhibit ductile failure on GIA timescales (see Fig. 4 and related discussion). The continuous viscosity profiles shown in Fig. 1 are discretized with a depth resolution of ~1 km for the purpose of computing viscoelastic Love numbers (Peltier, 1974).

Barnhoorn et al. (2011) suggest ~10^{25} Pa s as a good minimum viscosity value in the lithosphere to ensure elastic deformation on GIA timescales. We note that only very small sections of our ductile models have values above this minimum and so we expect that our models (Fig. 1) have an effective elastic thickness that is much thinner than their defined thickness would suggest.

2.2. Modelling approach

Changes in RSL have provided the most robust constraints on Earth viscosity structure in previous GIA modelling studies (e.g., Lambeck et al., 1996; Paulson et al., 2007). We therefore consider predictions of RSL at a small suite of sites around the globe where data have been obtained and used to infer lithospheric thickness. Six of the eight localities were chosen (sites 1–6 in Fig. 3a) due to their location relative to ancient ice sheets of a given size; from largest to smallest considered: Laurentian (1 & 2); Fennoscandian (5 & 6) and British-Irish (3 & 4). In each of these site pairs, one

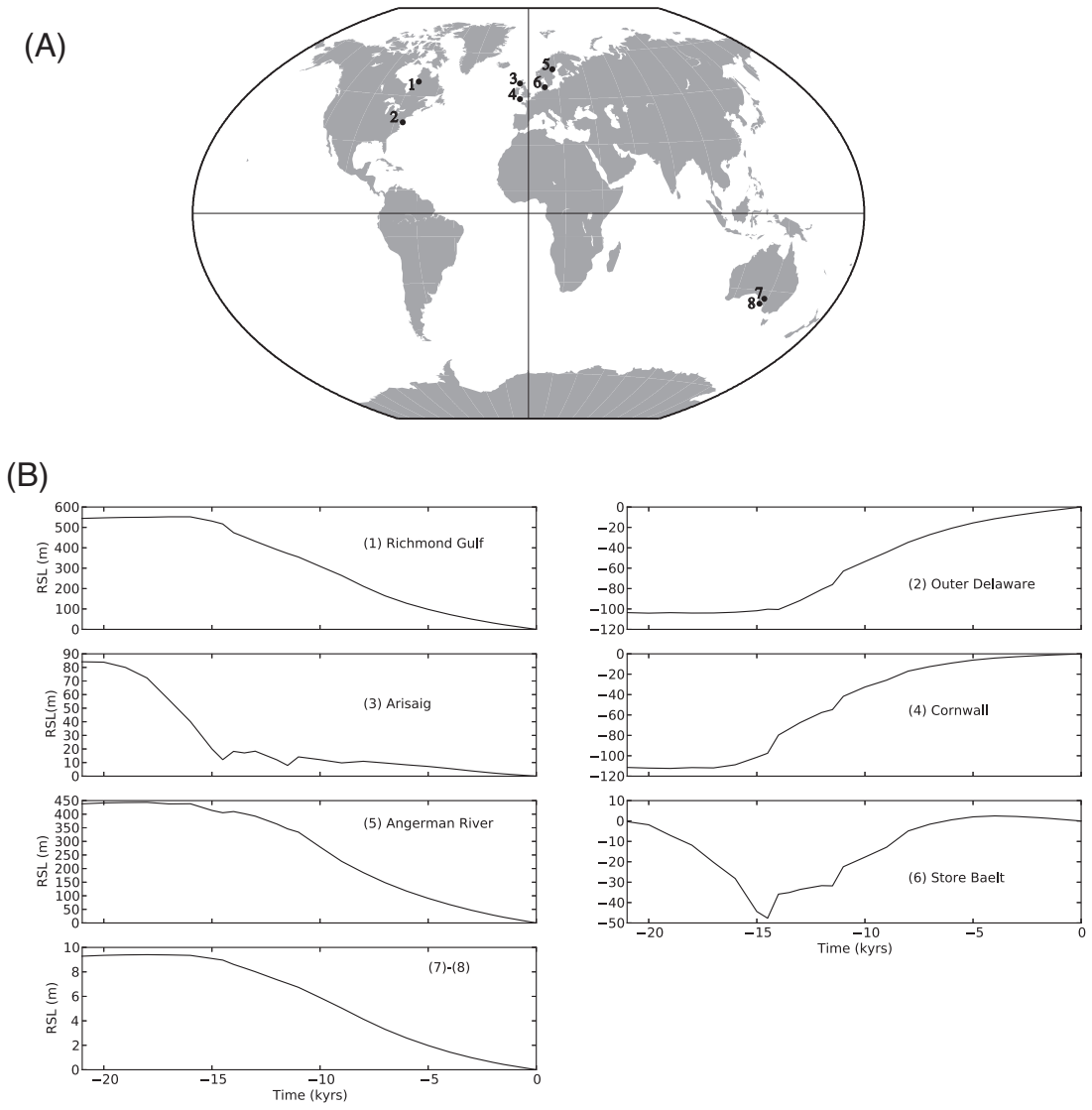

Fig. 3. (A) The sites considered in this study, from 1 to 8, are Richmond Gulf, Outer Delaware, Arisaig, Cornwall, Angerman River, Store Baelt, Port Pirie, and Cape Spencer (see Section 3). (B) An example of RSL curves for each of the sites, along with the difference in RSL between Port Pirie and Cape Spencer (see Section 3) for a 96 km elastic plate lithosphere model.

site is located near the centre of the, now melted, ice sheet and the other close to the margin. By considering a range of ice sheet size as well as locality of the sites with respect to the ice sheet, different depth sensitivities to viscosity structure are sampled. In this analysis, sensitivity to shallow (lithosphere) structure is the primary focus. The other two sites (7 & 8) are located distant from major glaciation centres, where the RSL signal is driven primarily by ocean loading (hydro-isostasy). These sites, and particularly the RSL difference between the two sites, have provided powerful constraints on viscosity structure (e.g., Nakada and Lambeck, 1989).

To complement the RSL predictions outlined above, we also generated model output of land height change produced by a simple parabolic load that is placed on the model Earth and does not vary in time. These model results, shown at the beginning of the following section, enable a more straightforward interpretation of the difference in output between the two lithosphere models (with and without viscous structure).

3. Results and discussion

In Fig. 4 we show the modelled deformation of the Earth under a time invariant parabolic ice load. We compare the deformation of D123 and D95 with the deformation of the suite of high viscosity lithosphere models by plotting the vertical deformation radially from the centre of the ice load, and we consider small (radius 1°, maximum thickness 100 m) and large (radius 15°, maximum thickness 3000 m) loads. We denote the high and uniform viscosity lithosphere models by their thickness with a prefix E (i.e., E71, E96, and E120) since the thickness reflects the EET in this case.

When we compare the deformation of D123 and D95 with the elastic models it is evident that any conclusion we may make about the effective thickness of the lithosphere for the ductile models is dependent on both the size and age of the load. Examining the vertical displacement near the loading centre for the larger ice load, when the ice load has been left for 2 kyr, the deformation of D123 is similar to that of E120; while for the smaller ice load the deformation of D123 at this time step is slightly less than that of E96. After the load has been left for 20 ka, comparison between the two sets of models indicates that the EET of the ductile models has thinned considerably relative to the elastic lithosphere models. For example, in the larger load test, the deformation near the centre of the load for D123 is similar to that for E96, whereas, for the smaller load, the result for E71 is about midway between D123 and D96. This is a result of viscous flow in the lower viscosity ductile models.

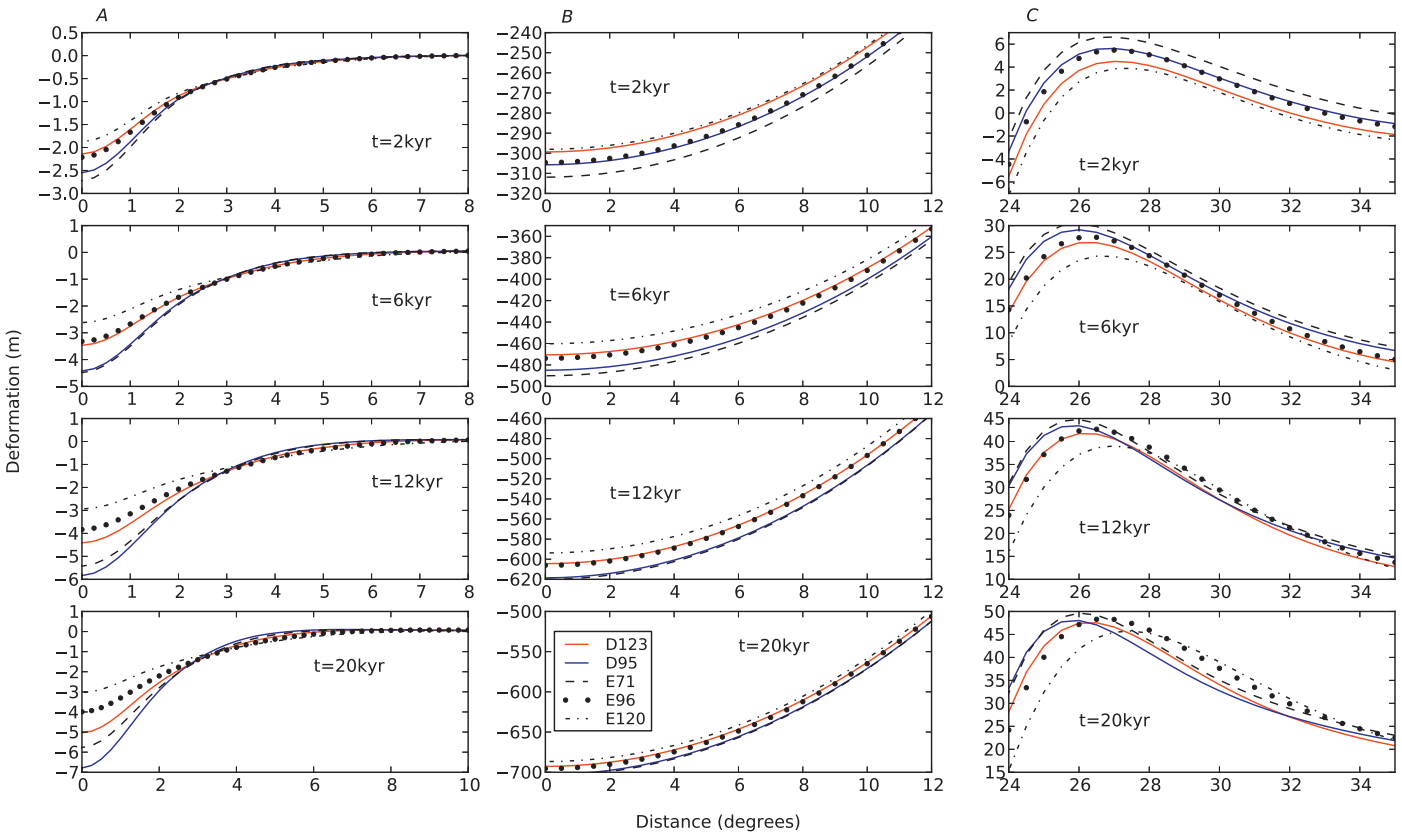

Fig. 4. Vertical displacement of the model Earth surface for a parabolic ice load along a radial transect from the centre of the ice sheet. In column A we show the vertical displacement for a small ice load (radius 1°, maximum thickness 100 m), while columns B and C show the deformation at the load centre (B), and peripheral bulge (C), for a relatively large (radius 15°, maximum thickness 3000 m) ice load.

The enhanced thinning in the case of the smaller load reflects its shallower depth sensitivity.

Towards the edge of the load and beyond, there are also some interesting differences between the two types of lithosphere model. However, the comparison is complicated by lateral migration of the peripheral bulge. This is most evident in the results for the smaller load as the bulge is completely captured in Fig. 4 (left column). For a given lithospheric thickness, the lateral movement of the bulge becomes more pronounced with time in the 'D' models compared to the 'E' models as the EET thins leading to some interesting differences. For example, the vertical deflection profiles in Fig. 4 for the 15° radius load demonstrate that directly at the bulge, D123 closely matches E96 at 20 kyr, as it does under the load. However, further away from the load D123 no longer tracks E96, and instead seems to suggest its behaviour there would be analogous to a lithosphere even thinner than E71. Indeed, there is no overlap between E123/96/71 and D123/95 moving away from the load centre beyond the peripheral bulge.

The above comparison demonstrates increasing amounts of viscous flow in the lithosphere with time and therefore a reduction in the EET in the ductile models. However, it is important to note that since we assume a linear Maxwell rheology in the numerical computations, the influence of changing stress with time is not modelled.

The results in Fig. 4 show the response of an idealised ice load. We will now consider RSL predictions from a more realistic loading history (provided by ICE5G, version 1.2; Peltier, 2004). By RSL we mean the height between the bedrock and the geopotential surface that defines sea level. In order to determine how the RSL predictions based on the more realistic lithosphere models differ from those of the elastic models for a more realistic ice history, we generated results for the 8 locations described in Section 2. Before going on to examine the difference in output for the two types of lithosphere model, it is useful to first look at the predicted RSL curves for each location. Relative sea level curves at these sites for a traditional 96 km elastic lithosphere model are displayed in Fig. 3b. For the sites in Australia we have shown the difference between the two sites, which is more sensitive to lithosphere variation than the RSL curves for individual sites on their own (Nakada and Lambeck, 1989).

Richmond Gulf and Angerman River (sites 1 and 5) show the largest responses, as they are located at the centre of where the Laurentide and Fennoscandian ice sheets were, respectively. The sea level fall shown for these sites is primarily caused by uplift. The Arisaig RSL curve is similarly dominated by land uplift, but the magnitude of the sea level fall is less than at Richmond Gulf and Angerman River because the British-Irish ice sheet was significantly smaller than the Laurentide and Fennoscandian ice sheets. We note also that Arisaig is located on the peripheral bulge of the Fennoscandian ice sheet, which contributes subsidence during the postglacial period. Sites like Outer Delaware in North America and Cornwall in southern UK are located outside the ice margin position during the last glacial maximum, on the peripheral bulge regions of, respectively, the North American and Eurasian ice complexes. The prediction for Store Baelt is the most complicated because the site is located near the hingeline of the Fennoscandian ice sheet and so the RSL curve displays an initial fall due to land uplift followed by a rise as the peripheral bulge migrates towards the location of the primary load centre. Finally, Port Pirie and Cape Spencer, in

Australia, are far from past centres of glaciation and so are more sensitive to ocean loading than ice loading. Due to their respective locations in Spencer Gulf, the RSL change at each site reflects a different response to the ocean loading: being further inland, Port Pirie is more strongly affected by continental levering (e.g., Clark et al., 1978) and thus exhibits a smaller RSL rise (due to enhanced land uplift) through the deglaciation. Hence, the difference between these sites is a monotonically decreasing signal with time that is dominated by the ocean loading signal.

Predicted RSL curves were generated for a suite of lithosphere models with and without viscous structure. To highlight differences between the results of these two models, we show in Fig. 5(A–D) predictions for D78, D95, D123, D174 minus those for E46 (A), E71 (B), E96 (C) and E120 (D). While the results from the simple parabolic loading models provide useful insight to the differences in the nature of the isostatic response between the two different types of lithosphere model, those in Fig. 5 provide a more accurate reflection of the implications for inferring lithospheric thickness from reconstructions of RSL. However, given the greater complexity of the load model (in terms of both time history and spatial extent), interpretation of the results in Fig. 5 is more difficult, particularly for sites significantly affected by peripheral bulge dynamics (as

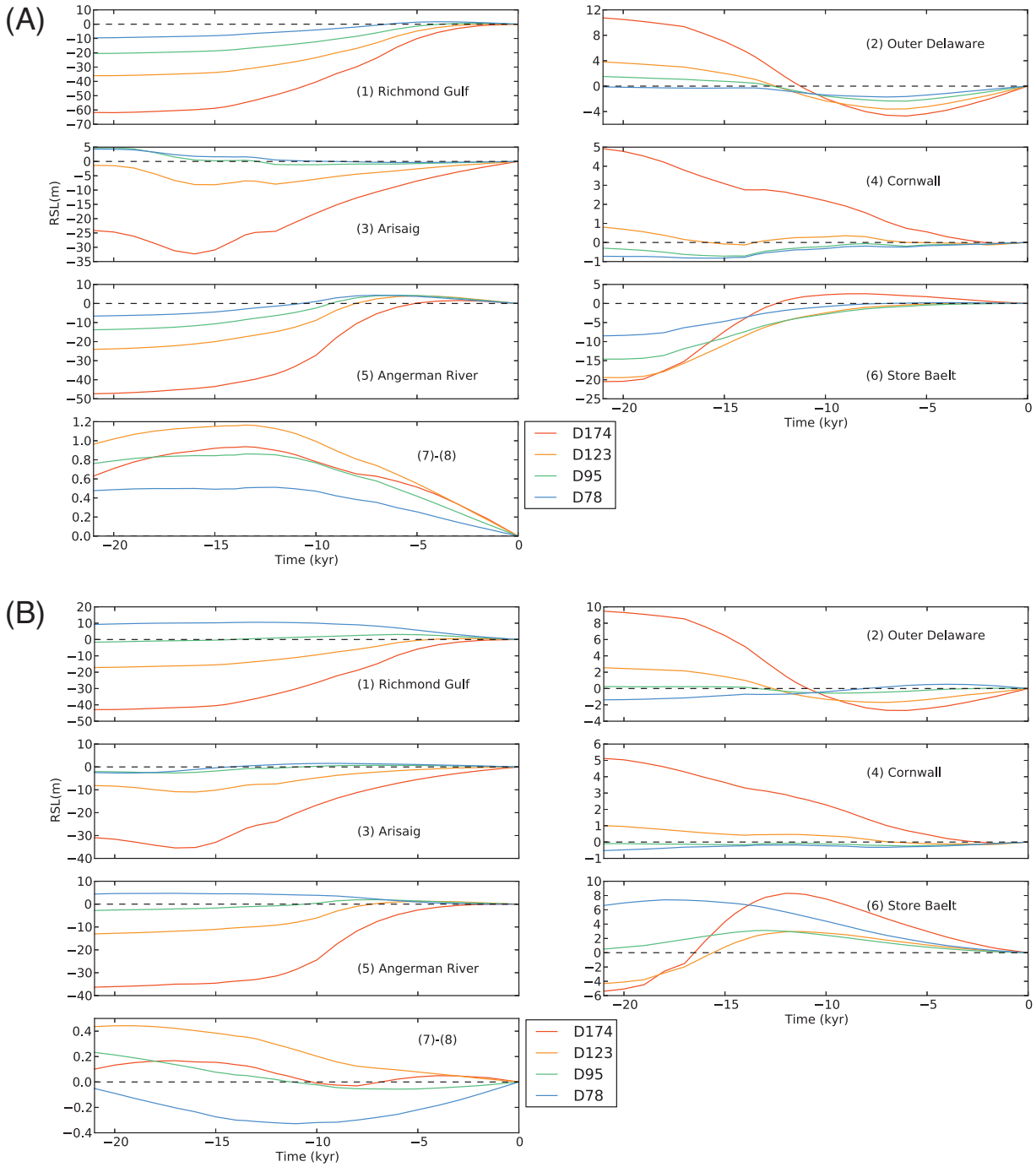

Fig. 5. Differences in RSL predictions between each of the more realistic lithosphere models (see colour key) and those of the (A) 46 km, (B) 71 km, (C) 96 km, and (D) 120 km elastic models. (For interpretation of the references to color in figure legend, the reader is referred to the web version of the article.)

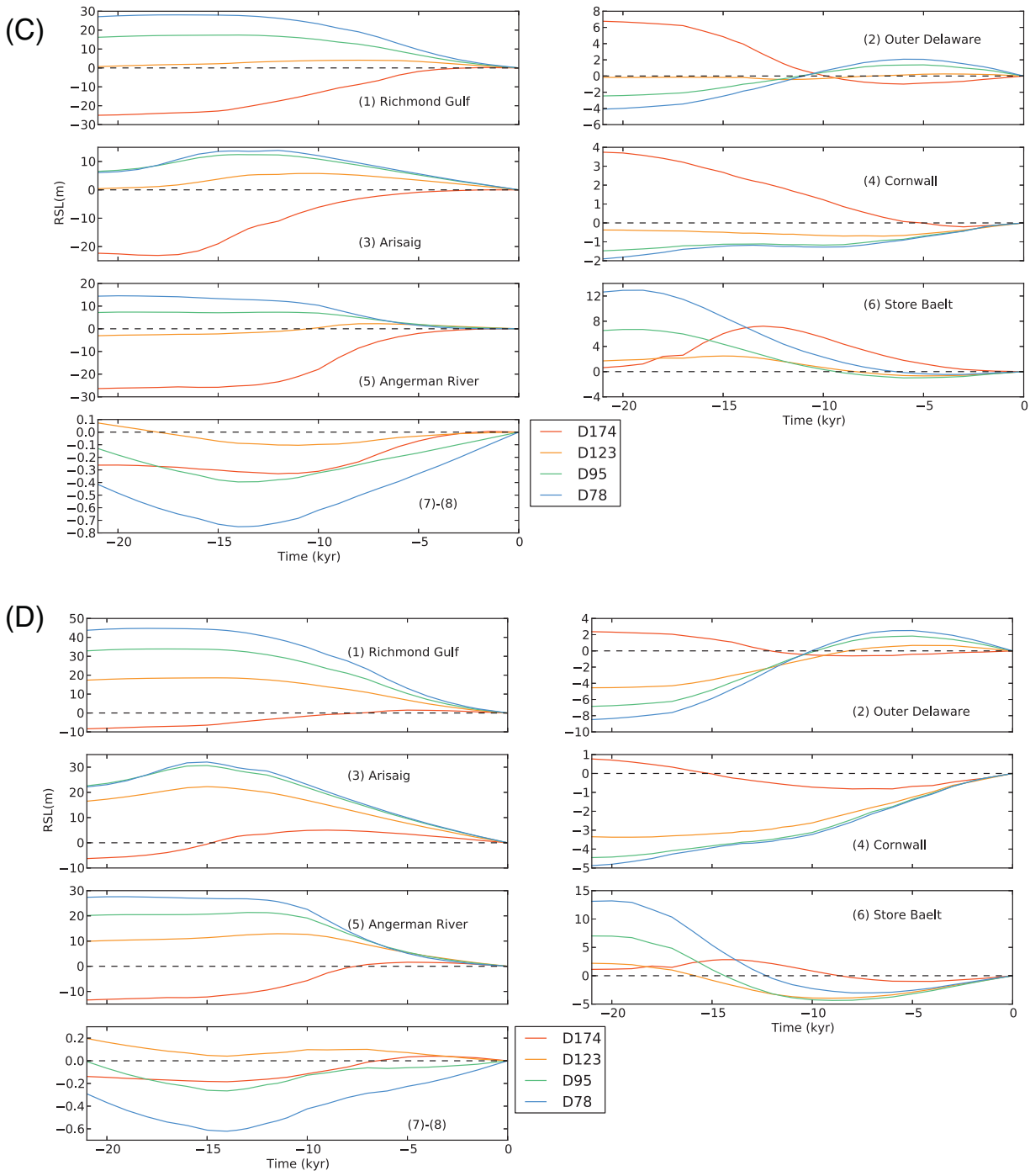

Fig. 5. (*Continued*).

indicated in Fig. 4). In particular, the tendency of the RSL differences to actually change sign and cross the zero-line at Outer Delaware, Cornwall and Store Baelt in Fig. 5(A–D) seems to be a reflection of this behaviour. This increased complexity is particularly true for Store Baelt and Cornwall; the former due to its proximity to the LGM margin of the Fennoscandian ice sheet and the latter because of the significant influence of both the British-Irish and Fennoscandian ice sheets (each with very different depth sensitivities and chronologies).

We found it to be often (but not exclusively) true that the predictions of any given elastic model were closest to the ductile model that was 20–30 km thicker. This is true in all cases for Richmond Gulf, Outer Delaware, and Angerman River, and it is frequently true for Store Baelt. This is consistent with the results from the parabolic ice load tests. However, we can see that for the sites in the British Isles, the predicted behaviours of D78 and D95 are very close to each other, often within a metre or less, and so it is not possible to say without ambiguity whether one ductile model would be preferable to another at this locality. Another interesting feature evident in the British Isles is that when comparing the ductile models to E96 (Fig. 5C), we can see that D123 provides the closest match to E96 early in the deglaciation up to about 10 ka BP, but nearer to the present it is D174 that tracks E96 the most closely. A possible explanation for this is that, as a relatively

small ice sheet, the deformation associated with the BIIS is more sensitive to shallower Earth structure than that caused by either the Laurentian or Fennoscandian ice sheets. The results for the Australian sites generally show the same overall behaviour of the closest match to a given elastic lithosphere model being the ductile lithosphere model 10–20 km thicker, with the exception of E120, which tends to be most similar to D123. In no cases (except Store Baelt, to an extent) do the results indicate that the best match for an elastic plate model is a significantly thinner ductile model.

The differences shown in Fig. 5 – those between the two model types and those between the different ductile models – reflect the ability of RSL data to infer lithospheric thickness. The precision of sea-level reconstructions ranges from sub-metre to several metres depending on the indicator(s) available at a given location and time (e.g., Elias, 2013; see contributions to section titled "Sea Level Studies"). Since the majority of data span the Holocene (past ~12 kyr) only, our results indicate that existing data are capable of resolving between several but not all (e.g., D95 and D71 at some sites) of the models considered in Fig. 5. However, this statement does not consider the issue of parameter trade-off which will limit the ability of RSL data to constrain lithospheric thickness given uncertainty in the loading history and sub-lithosphere viscosity.

4. Conclusion

We incorporated realistic viscosity structure in the lithosphere in the Earth component of a GIA model. We find that the RSL predictions of a given lithosphere model with viscous structure are, in general, most similar to those of an elastic model with a significantly thinner lithosphere. We conclude that the application of elastic lithosphere models in previous GIA analyses generally results in an underestimation of lithosphere thickness by tens of kilometres compared to models with viscous structure in the lithosphere. The greatest sensitivity to the imposed changes in lithosphere viscosity structure is evident in the British Isles, where there was a relatively small ice sheet and in Store Baelt which is located near the hingeline of the Fennoscandian ice sheet. We also investigated the time dependence of vertical deformation and found that for short time scales (~2 kyr), the response of a model with lithosphere structure is similar to that of an elastic plate of similar thickness, but that it effectively thins by tens of kilometres over a time scale of ~10 kyr.

While this work does not fully bridge the gap between lithosphere thickness estimates derived through GIA modelling as opposed to through other means, it does close the gap and thus provides a part explanation for the difference. For example, while seismic studies of the British Isles have determined a distance to the lithosphere-asthenosphere boundary of 110–150 km, GIA studies tend to find best fitting Earth models with ~70 km thick lithospheres. Comparing predictions of a 71 km elastic plate lithosphere model to our more realistic models, the predictions in Arisaig and Cornwall are comparable to either the 78 km or 95 km ductile models for time up to about 10 kyr BP, or the 123 km ductile model after 10 kyr BP and approaching the present.

An important avenue for future work is to incorporate non-linear (power law) flow into the type of analysis presented above. Allowing non-linear flow would cause the (effective) viscosity in the model to change in time. This process could act in an opposite sense to the EET thinning indicated in our results as stresses are maximum at the onset of loading and progressively relax as deformation proceeds.

Acknowledgements

JK would like to acknowledge funding from the University of Ottawa and through the Ontario Graduate Scholarship program. GAM acknowledges funding from the Natural Science and Engineering Research Council of Canada, the Canada Research Chairs program, the Canadian Foundation for Innovation and the University of Ottawa. We thank Jerry Mitrovica for discussions that contributed to the results presented in this paper.

References

Audet, P., Mareschal, J.C., 2004. Variations in elastic thickness in the Canadian Shield. Earth Planet. Sci. Lett. 226, 17–31.
Barnhoorn, A., van der Wal, W., Vermeersen, B.L.A., Drury, M.R., 2011. Lateral, radial, and temporal variations in upper mantle viscosity and rheology under Scandinavia. Geochem. Geophys. Geosyst. 12.
Bradley, S.L., Milne, G.A., Teferle, F.N., Bingley, R.M., Orliac, E.J., 2009. Glacial isostatic adjustment of the British Isles: new constraints from GPS measurements of crustal motion. Geophys. J. Int. 178, 14–22.
Bürgmann, R., Dresen, G., 2008. Rheology of the lower crust and upper mantle: evidence from rock mechanics, geodesy, and field observations. Annu. Rev. Earth Planet. Sci. 36, 531–567.
Clark, J.A., Ferrel, W.E., Peltier, W.R., 1978. Global changes in postglacial sea level: a numerical calculation. Quat. Res. 9, 265–287.
Davis, J.L., Mitrovica, J.X., 1996. Glacial isostatic adjustment and the anomalous tide gauge record of eastern North America. Nature 379, 331–333.
DiDonato, G., Mitrovica, J.X., Sabadini, R., Vermeersen, L.L.A., 2000. The influence of a ductile crustal zone on glacial isostatic adjustment: geodetic observables along the U.S. East Coast. Geophys. Res. Lett. 27, 3017–3020.
Dziewonski, A.M., Anderson, D.L., 1981. Preliminary reference earth model. Phys. Earth Planet. Inter. 25 (4), 297–356.
Elias, S. (Ed.), 2013. Encyclopedia of Quaternary Science. , 2nd ed. Elsevier, London, UK.
Kendall, R.A., Mitrovica, J.X., Sabadini, R., 2003. Lithospheric thickness inferred from Australian post-glacial sea-level change: the influence of a ductile crustal zone. Geophys. Res. Lett. 30, 14.1–14.4, http://dx.doi.org/10.1029/2003GL017022.
Kendall, R.A., Mitrovica, J.X., Milne, G.A., 2005. On post-glacial sea level-II. Numerical formulation and comparative results on spherically symmetric models. Geophys. J. Int. 161 (3), 679–706.
Klemann, V., Wolf, D., 1998. Modelling of stresses in the Fennoscandian lithosphere induced by Pleistocene glaciations. Tectonophysics 294, 291–303.
Klemann, V., Wolf, D., 1999. Implications of a ductile crustal layer for the deformation of the Fennoscandian ice sheet. Geophys. J. Int. 139, 216–226.
Kuchar, J., Milne, G., Hubbard, A., Patton, H., Bradley, S., Shennan, I., Edwards, R., 2012. Evaluation of a numerical model of the British-Irish ice sheet using relative sea-level data: implications for the interpretation of trimline observations. J. Quat. Sci. 27, 597–605.
Lambeck, K., Smither, C., Johnston, P., 1998. Sea-level change, glacial rebound and mantle viscosity for northern Europe. Geophys. J. Int. 134, 102–144.
Lambeck, K., Johnston, P., Smither, C., Nakada, M., 1996. Glacial rebound of the British Isles 2. Constraints on mantle viscosity. Geophys. J. Int. 125 (2), 340–354.
Levy, F., Jaupart, C., Mareschal, J.C., Bienfait, G., Limare, A., 2010. Low heat flux and large variations of lithospheric thickness in the Canadian Shield. J. Geophys. Res. 115.
Martinec, Z., Wolf, D., 2005. Inverting the Fennoscandian relaxation-time spectrum in terms of an axisymmetric viscosity distribution with a lithospheric root. J. Geodyn. 39, 143–163.
Milne, G.A., Mitrovica, J.X., 1998. Postglacial sea-level change on a rotating Earth. Geophys. J. Int. 133 (1), 1–19.
Mitrovica, J.X., Milne, G.A., 2003. On post-glacial sea level: I. General theory. Geophys. J. Int. 154 (2), 253–267.
Mitrovica, J.X., Wahr, J., Matsuyama, I., Paulson, A., 2005. The rotational stability of an ice-age Earth. Geophys. J. Int. 161, 491–506.
Nakada, M., Lambeck, K., 1989. Late Pleistocene and Holocene sea-level change in the Australian region and mantle rheology. Geophys. J. Int. 96 (3), 497–517.
Paulson, A., Zhong, S., Wahr, J., 2007. Inference of mantle viscosity from GRACE and relative sea level data. Geophys. J. Int. 171, 497–508.
Peltier, W.R., 1974. The impulse response of a Maxwell Earth. Rev. Geophys. 12, 649–669.
Peltier, W.R., Shennan, I., Drummond, R., Horton, B., 2002. On the postglacial isostatic adjustment of the British Isles and the shallow viscoelastic structure of the Earth. Geophys. J. Int. 148, 443–475.
Peltier, W.R., 2004. Global glacial isostasy and the surface of the ice-age Earth: the ICE5G (VM2) model and GRACE. Ann. Rev. Earth Planet. Sci. 32, 111–149.
Ranalli, G., 1995. Rheology of the Earth, 2nd ed. Chapman and Hall, pp. 230.
Sella, G.F., Stein, S., Dixon, T.H., Craymer, M., James, T.S., Mazzotti, S., Dokka, R.K., 2007. Observation of glacial isostatic adjustment in stable North America with GPS. Geophys. Res. Lett. 34, L02306.

Tesauro, M., Kaban, M.K., Cloetingh, S.A.P.L., 2009. A new thermal and rheological model of the European lithosphere. Tectonophysics 476, 478–495.
Turcotte, D.L., Schubert, G., 2002. Geodynamics, 2nd ed. Cambridge University Press.
van der Wal, W., Barnhoorn, A., Stocchi, P., Gradmann, S., Wu, P., Drury, M., Vermeersen, L.L.A., 2013. Glacial isostatic adjustment model with composite 3D earth rheology for Fennoscandia. Geophys. J. Int., http://dx.doi.org/10.1093/gji/ggt099.
Watts, A.B., Zhong, S.J., Hunter, J., 2013. The behaviour of the lithosphere on seismic to geologic timescales. Annu. Rev. Earth Planet. Sci. 41, 443–468.
Wu, P., Wang, H., 2008. Postglacial isostatic adjustment in a self-gravitating spherical earth with power-law rheology. J. Geodyn. 46, 118–130.